Dyes and Pigments 112 (2015) 317–326

Contents lists available at ScienceDirect

Dyes and Pigments

journal homepage: www.elsevier.com/locate/dyepig

Synthesis and intramolecular FRET of perylenediimide–naphthalimide dendrons

Huan-ren Cheng, Ying Qian*

School of Chemistry and Chemical Engineering, Southeast University, Nanjing 211189, China

ARTICLE INFO

Article history:
Received 24 May 2014
Received in revised form
1 July 2014
Accepted 4 July 2014
Available online 4 August 2014

Keywords:
Fluorescence resonance energy transfer
Photoinduced electron transfer
Perylenediimide
Naphthalimide
Fluorescent probes
Dendrons

ABSTRACT

Two novel fluorescence resonance energy transfer-based perylenediimide–naphthalimide dendrons with perylenediimides as the energy acceptor, tertiary amines as the proton or metal receptor and naphthalimide as the energy donor were successfully synthesized. The dendrons exhibited high selectivity toward Fe(III) in the presence of various other metal cations and exhibited sensitivity to protons. A 1:2 stoichiometry was found for the complex formed by the probes and Fe(III) using a Job's plot and by non-linear least square fitting of the fluorescence titration curves. The probe molecules present abilities of fast fluorescence detection of Fe(III) and for the fluorescent detection of protons with high energy transfer efficiency of 96–98%.

1. Introduction

Perylene tetracarboxylic diimides (**PDI**s) have recently generated great interest in the field of photonic materials, because of their excellent photo-stability, high luminescence efficiency, and novel optoelectronic properties [1–3]. Perylenediimide dendrons have attracted much attention because of their unique structures which enable them to concentrate a high number of end groups in one molecule. Perylenediimide dendrons have wide applications in optical materials, photosynthetic models and chemosensors [4–7]. For example, Akkaya et al. reported a boron-dipyrrin functionalized perylenediimide derivative with an energy transfer efficiency as high as 99% [8]. **PDI** are also good electron acceptors with a low reduction potential [9–12]. Several **PDI** probes should be promising candidates for fluorophores in fluorescent probes based on photoinduced electron transfer (PET). Recently several PDIs probes based on PET mechanism have been developed [13–20]. Shen et al. reported a multifunctional perylenediimide derivative, which can be used as a recyclable specific Hg^{2+} ion sensor [21]. However, fluorescence resonance energy transfer (FRET) and PET-based dendritic perylenediimide fluorometric probes are still at a modest number [22].

Most perylenediimide fluorometric sensors are designed to sense photophysical changes produced upon complexation, including photoinduced electron transfer (PET), photoinduced charge transfer (PCT) [7] and fluorescence resonance energy transfer (FRET) [23]. Among numerous mechanisms, PET has been widely used in the design of new sensors. A “turn-on” motif based on PET, which changes from a non-fluorescent state to a fluorescent state upon analyte binding, is widely employed in many perylenediimide fluorometric sensors due to the inherently higher sensitivity of PET as compared to the normal fluorescence quenching motif [24–27]. Known to be sensitive, selective, and adaptable to a wide variety of systems [28,29], FRET plays a more significant role in natural photosynthetic process where solar energy is captured and delivered to the reaction center to initiate a multistep electron-transfer cascade.

To make a useful probe, a compound must possess two functional units: an ionophore responsible for selectively binding ions and a fluorophore responsible for signal transduction [30–34]. Furthermore, a communication mechanism between the binding and signaling sites must exist [35]. In this work, we exploited an excellent ratiometric Fe(III) probe based on a Fe(III) complex with nonconjugated “energy donor–spacer–receptor” structure as shown in Fig. 1, and further investigated the effect of N–Fe(III) binding on the energy transfer from donor to acceptor. Herein, we synthesized two compounds with perylenediimide as energy acceptor, 1, 8-naphthalimide derivative as peripheral fluorophore

* Corresponding author. Tel.: +86 25 83793591; fax: +86 25 83795857.
E-mail address: yingqian@seu.edu.cn (Y. Qian).

http://dx.doi.org/10.1016/j.dyepig.2014.07.005
0143-7208/

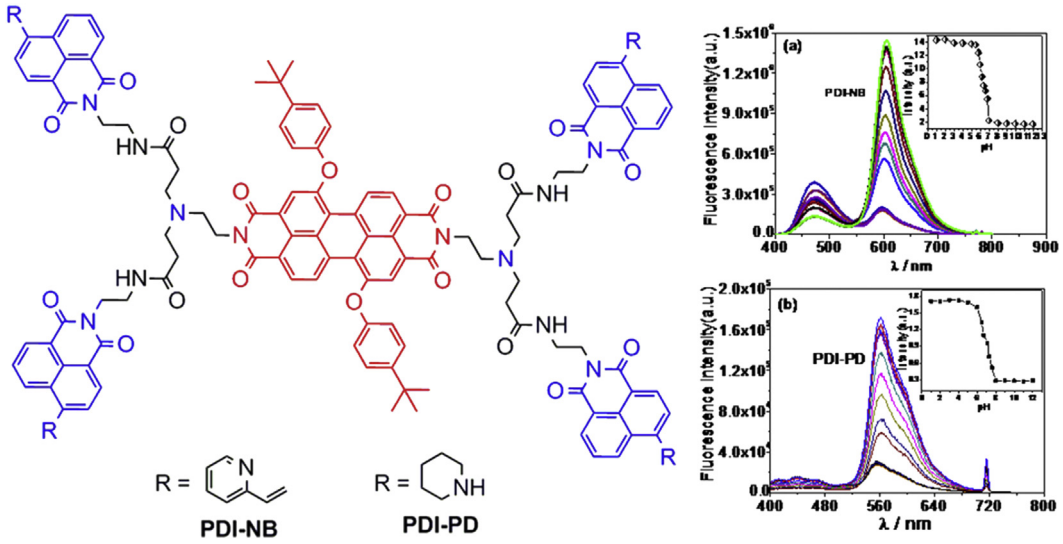

Fig. 1. Structures of the light-harvesting molecules **PDI-PD** and **PDI-NB** (Inset: Fluorescence spectra of **PDI-NB** (a) and **PDI-PD** (b) at various pH values).

and poly(amidoamine) (PAMAM) as linker. In addition, several reference compounds (shown in Scheme 1), such as complex **NB**-1, fluorescent donor, and fluorescent acceptor **PDI-2**, were also synthesized in order to better understand the combined influence on the excited-state properties of the complexes. Finally, the binding of Fe(III) to **PDI-NB** or **PDI-PD** changes the excited-state properties of the acceptor, inducing variation in FRET (fluorescence resonance energy transfer) from donor to acceptor, and makes an excellent ratiometric probe for Fe(III) and proton with switchable fluorescence signals.

2. Experimental

2.1. Experimental section

2.1.1. Materials and methods

^{1}H NMR and ^{13}C NMR spectra were recorded on a Bruker DMX 300 NMR spectrometer and a Bruker ADVANCE 500 NMR spectrometer in $CDCl_3$ with tetramethylsilane (TMS) as internal standard. Chemical shifts are given in parts per million (ppm). Mass spectra were recorded on Agilent Technologies 6530 Accurate-Mass Q-TOF LC/MS. HRMS were recorded on an Ultraflex II MALDI-TOF mass spectrometer. UV–visible absorption spectra were determined on a Shimadu UV-3600 spectrophotometer. Fluorescence spectra were measured on a HORIBA FL-4 Max spectrometer. Fluorescence life time was measured on an Edinburgh FLS920 spectrometer. FT-IR spectra were recorded on a Nicolet 750 series in the region of 4000–400 cm^{-1} using KBr pellets. All reagents used were purchased from Aldrich, Fluka or Alfa Aesar and used without further purification. All solvents used in spectroscopic measurements were of analytical grade. Reactions were monitored by thin layer chromatography using Merck TLC Silica gel 60 F254. Silica gel column chromatography was performed over Merck Silica gel 60.

2.1.2. Synthesis

*2.1.2.1. Compound **2**.* Compound **2**, **3** and **AN-Boc** were prepared in the published method [36].

A dichloromethane solution (500 mL) of di-tertbutyl dicarbonate(8 g, 36.7 mmol) was added dropwise over 6 h to vigorously stirred dichloromethane (50 mL) solution of ethylenediamine (13.2 g, 220 mmol) at 0 °C. The reaction mixture was then left stirring overnight. The solvent was removed under a reduced pressure to give an oily liquid which was then dissolved in doubly distilled water (100 mL), filtered, and then extracted with dichloromethane (2 × 300 mL). The final product obtained was a viscous, colorless oil **2** (5.22 g). Yield: 88%. ^{1}H NMR ($CDCl_3$, ppm): δ 5.24 (s, 1H, Boc-NH–), 3.10–3.07 (m, 2H, –NH–CH_2–), 2.71–2.67 (m, 2H, –CH_2–NH_2), 1.35 (s, 9H, $(CH_3)_3$–). TOF-MS-ES: *m/z*. Calculated: $([M+H])^+ = 161.1$, found: 161.2.

*2.1.2.2. Compound **3**.* N-Boc-ethylenediamine **2** (5 g, 31 mmol) was dissolved in methanol (150 mL); to this methyl acry-late (26.9 g, 310 mmol) dissolved in methanol (50 mL) was added slowly. The reaction mixture was left stirring for 3 days at room temperature. The solvent and excess methyl acrylate were removed under reduced pressure at 60 °C using a rotary evaporator. A more rigorous purification was then carried out via column chromatography (ethyl acetate) to give **3** (10 g), Yield: 97%. ^{1}H NMR ($CDCl_3$, ppm): δ 5.13 (s, 1H, Boc-NH–), 3.69 (s, 6H, O–CH_3), 3.2–3.14 (m, 2H, NH–CH_2), 2.77–2.73 (t, 4H, –N–(CH_2–)$_2$, J = 6.6 Hz), 2.54–2.52 (t, 2H, –CH_2–N–(CH_2–)$_2$, J = 6.0 Hz), 2.50–2.41 (t, 4H, –CH_2–CO_2Me, J = 6.6 Hz), 1.44 (s, 9H, $(CH_3)_3$–).

*2.1.2.3. Compound **AN-Boc**.* Compound **3** (5 g, 15 mmol) was dissolved in methanol (50 mL) then was added slowly to a cooled (0 °C) methanol solution of ethylenediamine (30 g, 500 mmol). The reaction mixture was left stirring for 5 days at room temperature.

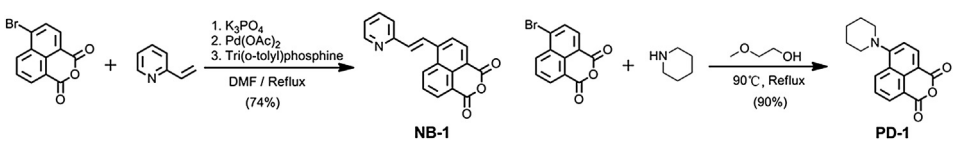

Scheme 1. Synthesis of the modules **NB-1** and **PD-1**.

The solvent and the majority of the excess ethylenediamine were removed under reduced pressure at 60 °C using a rotary evaporator, with a rigorous purification being carried out by using a heated vacuum desiccator and a high vacuum mineral oil vacuum pump (60 °C) and a high vacuum mineral oil vacuum pump. The product obtained was a thick, viscous honey-like oil (5.7 g). Yield: 99%. ^{1}H NMR ($CDCl_3$, ppm) δ 7.51 (s, 2H, CO–N<u>H</u>–CH_2–), 6.14 (t, 1H, Boc-N<u>H</u>–), 3.11–3.06 (q, 4H, –C<u>H</u>$_2$–CH_2–NH_2), 2.99–2.95 (q, 2H, Boc-NH–C<u>H</u>$_2$–), 2.65–2.61 (t, 4H, –CH_2–C<u>H</u>$_2$–NH_2), 2.56–2.53 (t, 4H, –N–(C<u>H</u>$_2$–)$_2$), 2.35–2.32 (t, 2H, –C<u>H</u>$_2$–N–(CH_2–)$_2$), 2.17–2.14 (t, 4H, –C<u>H</u>$_2$–CO–NH–), 1.24 (s, 9H, (C<u>H</u>$_3$)$_3$–). TOF-MS-ES: *m*/*z*. calculated: $[M+H]^+$ = 389.2, Found: 389.3.

2.1.2.4. Compound ***PD-1***. Compound **v-1** was prepared as the published method [37].

A mixture of 4-Bromo-1,8-naphthalicanhydride (10 g, 36.2 mmol) and piperidine (3.69 g, 43.5 mmol) in 100 mL 2-methoxyethanol was heated under reflux for 12 h under N_2. After cooled to room temperature, 100 mL water was joined, a majority of yellow solid separate out, filtrated and then recrystallized by ethanol. A bright yellow solid got. 9.2 g, Yield: (90%). ^{1}H NMR ($CDCl_3$, ppm): δ 8.53–8.51 (d, 1H, H-6, J = 6.0 Hz), 8.45–8.41 (t, 2H, J = 6.0 Hz, H-10, 8), 7.7–7.65(t, J = 9.0 Hz, 1H, H-9), 7.19–7.16 (t, 1H, J = 9.0 Hz, H-7), 3.31–3.28 (m, 4H, C<u>H</u>$_2$–N–C<u>H</u>$_2$, J = 6.0 Hz), 1.90–1.89 (m, 4H, C<u>H</u>$_2$$CH_2$C<u>H</u>$_2$), 1.77–1.75 (m, 2H, CH_2C<u>H</u>$_2$$CH_2$). MALDI-TOF-MS: *m*/*z*. Calculated: $[M+H]^+$ = 281.1, Found: 282.1, ($[M+Na]^+$) 314.1.

Synthesis of 1,7-bis(4-tert-butylphenyloxy)perylene-3,4:9,10-tetracarboxylic acid bisanhydride (**PDI-2**) [38].

A mixture of 1,7-dibromoperylene-3,4:9,10-bis (dicarboxylic anhydride) (2.0 g, 3.6 mmol), 4-tert-butylphenol (1.8 g, 12.0 mmol), and cesium carbonate (2.38 g, 6.8 mmol) in dry DMF (120 mL) was heated at the refluxing temperature for 4 h under an N_2 atmosphere. The reaction mixture was poured into water (100 mL) and neutralized with aqueous 1.2 N HCl solutions. The formed precipitate was collected by filtration and washed with water and methanol to give crude PDI-2 in 92% as this product showed poor solubility in common organic solvents. Without further purification it was used to the next reaction.

2.1.2.5. Compound ***NB-1***. A mixture of $Pd(OAc)_2$ (22.5 mg, 0.10 mmol), tri(o-tolyl)Phosphine (70.5 mg, 0.20 mmol), K_3PO_4 (1.84 g, 5 mmol), 2-vinylpyridine (0.91 g, 8.69 mmol), and 4-Bromo-1,8-naphthalicanhydride (2 g, 7.24 mmol) in DMF (100 mL) was stirred for 24 h at 130 °C, under N_2. After cooled to room temperature H_2O (150 mL) were added to the reaction mixture. The precipitation was filtrated and washed with water and then recrystled by methanol. A yellow solid got. 1.61 g, Yield: (74%). ^{1}H NMR ($CDCl_3$, ppm): δ 8.85–8.82 (d, 1H, J = 9.0 Hz, H-1), 8.77–8.75 (d, 1H, J = 6 Hz, H-5), 8.73 (s, 0.5H, H-3), 8.71–8.69 (d, 1H, J = 6.0 Hz, H-9), 8.67 (s, 0.5H, H-3), 8.62 (s, 0.5H, H-4), 8.57 (s, 0.5H, H-4), 8.17–8.14 (d, 1H, J = 9 Hz, H-2), 7.93–7.88 (m, 1H, H-6), 7.83–7.77 (m, 1H, H-7), 7.52 (s, 0.5H, H-8), 7.49–7.48 (d, 1H, J = 6 Hz, HC=C), 7.43 (s, 0.5H, H-8), 7.34–7.32(d, 1H, J = 6 Hz, C=CH). TOF-MS-ES: *m*/*z*. Calculated: 301.0, Found: $[M+H]^+$ = 302.1, $[M+Na]^+$ = 334.1.

2.1.2.6. Compound ***NB-2***. A mixture of compound **AN-Boc** (0.8 g, 2.06 mmol), compound **NB-1** (1.39 g, 4.94 mmol) was dissolved in anhydrous ethanol (150 mL), refluxed for 48 h, after reaction was finished (by TLC track), the ethanol was removed using a rotary evaporator, The residue was subjected to silica gel column chromatography (eluting with DCM: methanol = 10:1) to give a yellow solid (m.p. 142–144 °C). 1.54 g, Yield: (78%). FT-IR (KBr) cm^{-1}: 3382 and 3294 (νNH); 2978–2924(νCH); 1698(ν^{as}N–C=O); 1657(ν^{s}N–C=O); 1576(νN-C=O). ^{1}H NMR ($CDCl_3$, ppm): δ 8.65–8.63 (d, 2H, H-1), 8.32–8.29 (d, 2H, J = 9 Hz, H-5), 8.25–8.22 (d, 4H, J = 9 Hz, H-3, H-9), 8.13–8.08 (d, 2H, J = 15 Hz, <u>H</u>$_2$C=C), 7.71–7.67 (m, 3H, H-2, 4), 7.65–7.60 (d, 2H, H-6), 7.51–7.46 (t, 2H, CO–N<u>H</u>–CH_2–), 7.34–7.32(t, 2H, H-7), 7.22–7.20 (t, 2H, H-8), 7.13–7.08 (d, 2H, J = 15 Hz, C=C<u>H</u>$_2$), 5.67 (t, 1H, Boc-N<u>H</u>–), 4.19 (t, 4H, –C<u>H</u>$_2$–N–(CO–)$_2$), 3.65–3.66 (q, 4H, –CO–NH–C<u>H</u>$_2$–), 3.24 (q, 2H, Boc-NH–C<u>H</u>$_2$–), 2.65 (s, 4H, –N–(C<u>H</u>$_2$–)$_2$), 2.51 (t, 2H, –C<u>H</u>$_2$–N–(CH_2–)$_2$), 2.33 (t, 4H, –C<u>H</u>$_2$–CO–NH–), 1.41 (s, 9H, (C<u>H</u>$_3$)$_3$–). ^{13}C NMR ($CDCl_3$, ppm): δ 172.6, 164.3, 164.0, 156.0, 154.3, 149.9, 140.4, 133.7, 130.6, 129.9, 129.3, 128.1, 126.8, 126.5, 123.8, 123.3, 123.0, 122.2, 121.1, 52.6, 49.7, 39.9, 38.4, 33.2, 28.4. TOF-MS-ES: *m*/*z*. Calculated: 954.4, Found: $[M+H]^+$ = 955.4, $[M+Na]^+$ = 977.3.

Compound **PD-2** was prepared according the same method of compound **NB-2**, a yellow solid was got. Yield: (80%) (m.p. 132–134 °C). FT-IR (KBr) cm^{-1}: 3367 (νNH); 2937–2842(νCH); 1698(ν^{as}N–C=O); 1657(ν^{s}N–C=O); 1571(νN–C=O). ^{1}H NMR ($CDCl_3$, ppm): δ 8.39–8.37 (q, 0.65H, H-6), 8.33–8.31(d, 1.4H, H-6), 8.26–8.21 (q, 2H, H-10), 8.13–8.10 (q, 1.6H, H-8), 8.04–8.02 (d, 0.41H, H-8), 7.80–7.78 (q, 0.6H, H-9), 7.63–7.60 (q, 1H, H-9), 7.46–7.42 (q, 2.5H, N<u>H</u>), 7.31–7.26 (q, 0.41H, H-7), 6.97–6.92 (q, 1.4H, H-7), 5.59 (s, 1H, Boc-N<u>H</u>–), 4.22–4.18 (m, 4H, CO–NH–C<u>H</u>$_2$$CH_2$), 3.63–3.62 (m, 4H, –$CH_2$–N–(C<u>H</u>$_2$–)$_2$), 3.20 (s, 2H, –C<u>H</u>$_2$$CH_2$–N–($CH_2CH_2$)$_2$), 3.10–3.06 (m, 5.7H, CH_2C<u>H</u>$_2$–N–C<u>H</u>$_2$$CH_2$), 2.68–2.66 (m, 4H, CO–NH–CH_2·C<u>H</u>$_2$), 2.48 (s, 2H, –C<u>H</u>$_2$–N–(CH_2CH_2)$_2$), 2.29–2.23(m, 4H, –CH_2–N–(CH_2C<u>H</u>$_2$)$_2$). 1.83–1.82 (m, 6H, C<u>H</u>$_2$$CH_2$C<u>H</u>$_2$), 1.70–1.69 (m, 3H, CH_2C<u>H</u>$_2$$CH_2$), 1.39 (s, 9H, (C<u>H</u>$_3$)$_3$–). ^{13}C NMR ($CDCl_3$, ppm): δ 172.4, 164.6, 164.2, 157.1, 156.0, 132.8, 132.5, 131.6, 130.8, 130.7, 130.4, 130.3, 129.6, 127.7, 125.8, 125.0, 122.5, 114.4, 54.3, 52.7, 49.7, 39.6, 38.5, 33.5, 28.4, 26.1, 24.2. TOF-MS-ES: *m*/*z*. Calculated: 914.4, Found: $[M+H]^+$ = 915.4, $[M+Na]^+$ = 937.4.

2.1.2.7. Compound ***NB-3***. Compound vi-1 (1.2 g, 1.3 mmol) was placed into a round bottom flask to which dichloromethane (25 mL) and trifluoroacetic acid (6 mL) was added. The mixture was stirred vigorously and the reaction was followed by TLC (DCM: Methanol = 10:1). On completion of the reaction the excess trifluoroacetic acid and dichloromethane were removed under reduced pressure to give compound **BN-3**. Compound **BN-3** was used for the next reaction without further purification 98%. Compound **PD-3** was prepared according the same method of compound **PDI-NB**. Yield (99%).

2.1.2.8. Compound ***PDI-NB***. Compound **NB-3** (1.1 g, 1.2 mmol), compound **PDI-2** (0.42 g, 0.6 mmol) and $N(C_3H_7)_3$ was dissolved in DMF (30 mL), the mixture was heated under reflux for 12 h under N_2. After cooled to room temperature the solvent was removed under reduced pressure, a red-black solid got, washed with waters (150 mL), dry in 60 °C, A more rigorous purification was then carried out via column chromatography (eluting with DCM/Methanol = 20:1) to give a purple solid 0.9 g, Yield: 75%. (m.p. 208–210 °C). FT-IR (KBr) cm^{-1}: 3422 (νNH); 2950–2863(νCH); 1698(ν^{as}N–C=O); 1664(ν^{s}N–C=O) 1576(νN–C=O). ^{1}H NMR ($CDCl_3$, ppm): δ 9.25 (s, 2H, H-a, a′), 8.68 (s, 2H, H-1), 8.54–8.45(q, 4H, H-1, H-b, b′), 8.38–8.30(m, 6H, H-5, H-c, c′), 8.09–7.96(m, 9H, H-3, H-9, <u>H</u>$_2$C=C), 7.73–7.40(q, 20H, <u>H</u>$_2$C=C, CO–N<u>H</u>–CH_2–, H-2, 4, 6, 7), 7.14–7.09 (m, 9H, H-7, 8, H-d, d′), 6.99–6.95 (s, 4H, H-d, d′), 4.22–4.08 (m, 12H, 6 × (CONC<u>H</u>$_2$$CH_2$)), 3.62 (s, 8H, 4 × (CONCH_2·C<u>H</u>$_2$)), 2.86–2.72 (m, 12H, 2 × (C<u>H</u>$_2$N(C<u>H</u>$_2$$CH_2$)$_2$)), 2.40 (s, 8H, 2 × ($CH_2$N–($CH_2$C<u>H</u>$_2$)$_2$)), 1.37 (s, 18H, –C($CH_3$)$_3$). ^{13}C NMR ($CDCl_3$, ppm): δ 172.4, 172.3, 164.2, 154.0, 149.7, 139.9, 136.5, 133.3, 130.9, 130.4, 129.6, 127.5, 126.5, 123.5, 123.4, 123.2, 122.9, 119.1, 50.3, 50.2, 39.9. MALDI-TOF-MS: *m*/*z*. Calculated: $[M+H]^+$ = 2361.9039, found: 2361.9045.

Compound **PDI-PD** was prepared according the same method of compound **PDI-NB**. A oxblood red solid got. 1.61 g, Yield: 76%. (m.p. 180–182 °C). FT-IR (KBr) cm^{-1}: 3422 (νNH); 2971–2870(νCH); 1696(ν^{as}N–C=O) 1657(ν^{s}N–C=O) 1584(νN–C=O). ^{1}H NMR (CDCl3, ppm): δ 9.42–9.39 (m, 1H, H-1), 9.36–9.33 (q, 1H, H-1′), 8.41–8.33 (q, 4H, H-2, H-6), 8.27–8.25 (m, 2H, H-6), 8.20 (s, 1H, H-10), 8.17–8.12 (m, 4H, H-10, 8), 8.09 (q, 1H, H-8), 8.06 (m, 1H, H-8), 8.04–8.03 (m, 1H, H-9), 8.03 (m, 1H, H-9), 8.0–7.96 (m, 2H, H-9), 7.67–7.64 (m, 3H, H-10), 7.50–7.48 (m, 7.4H, $-CONHCH_2-$, H-10), 7.35–7.33 (m, 4H, H-5, 5′), 7.12–7.10 (m, 4H, H-4, 4′), 6.88–6.86 (m, 2.5H, H-3, 3′), 4.17–4.12 (m, 12H, 6 × ($CONCH_2CH_2$)), 3.54–3.53 (m, 8H, 4 × (CON CH_2CH_2)), 3.01 (m, 10H, $CH_2CH_2ArNCH_2CH_2$), 2.79–2.77 (m, 12H, 2 × (C $H_2N(CH_2CH_2)_2$)), 2.34 (m, 8H, 2 × ($CH_2N(CH_2CH_2)_2$)), 1.77–1.75 (m, 13H, $CH_2CH_2ArNCH_2CH_2$), 1.65–1.64 (m, 6H, $CH_2CH_2ArNCH_2CH_2CH_2$), 1.37 (s, 18H, $-C(CH_3)_3$). ^{13}C NMR (CDCl3, ppm): δ 172.2, 164.1, 163.5, 163.2, 157.0, 156.5, 152.3, 148.5, 146.0, 133.4, 132.2, 131.6, 131.0, 130.8, 130.2, 128.5, 127.7, 127.6, 125.7, 125.0, 124.9, 123.3, 123.2, 122.5, 122.3, 119.2, 114.4, 54.3, 39.6, 37.8, 33.8, 31.4, 26.2, 24.2. MALDI-TOF-MS: Calculated: *m/z*. $[M+H]^+$ = 2282.0291, Found: 2282.0297.

3. Results and discussion

3.1. Synthesis of perylenediimide–naphthalimide dendrons

The novel perylenediimide–naphthalimide dendrons were prepared in three parts (Schemes 1 and 2): synthesis of the functional naphthalimide, PAMAM dendronization of the functional naphthalimide to an amino-terminated naphthalimide PAMAM dendron and peripheral decoration of the perylenediimide with latter to the perylenediimide–naphthalimide dendrons.

In brief, **NB-1** was synthesized using palladium-catalyzed Heck coupling of 4-Bromo-1,8-naphthalicanhydride with 2-vinylpyridine. Then, **NB-2** was prepared via amidation reaction of **NB-1** with **AN-Boc**, which carries two terminal 8-vinylpyridine naphthalimide units. After purification by column chromatography, the amino protecting group Boc of **NB-2** was removed in trifluoroacetic acid, and used in the next reaction without purification. Reaction of **PDI-2** with a slight excess of **NB-3** in dry DMF in the presence of NEt_3 yielded **PDI-NB** with four shorter-wavelength 8-vinylpyridine naphthalimide units **NB-1**. It was purified by column chromatography (DCM/methanol = 9/1) to give a purple solid. **PDI-PD** was prepared according to the same method.

All of the new compounds were fully characterized by FT-IR, ^{1}H NMR, ^{13}C NMR and high-resolution mass spectrometry (HRMS-MALDI-TOF).

3.2. Absorption and fluorescence spectra of perylenediimide–naphthalimide dendrons

The dendritic naphthalimide–perylenediimide molecules **PDI-NB** and **PDI-PD** were configured on the "donor–spacer–receptor" model, where the perylene-diimide core is the fluorophore functioning as energy acceptor, the tertiary amines are the proton or metal receptor [36] and the naphthalimide is energy donor. The **AN-Boc** part between perylene-diimide core and naphthalimide fluorophore serves as spacer that covalently separates the two units. The maximum absorption spectra of **PDI-NB** were at 385 nm and 556 nm (Fig. 2(a)), and the maximum molar extinction coefficient (ε_{max}) of NB units was nearly 2.5 times that of NB-2 units in **PDI-NB**. The absorption spectra of **PDI-NB** indicates that the dendrimer holds the donor (yellow-green emitting periphery 1, 8-naphthalimide derivates) and the acceptor chromophores (red-emitting core **PDI-2**) together.

In these probes, it was predicted that a PET process (an electron transfers from the donor to the excited state of the

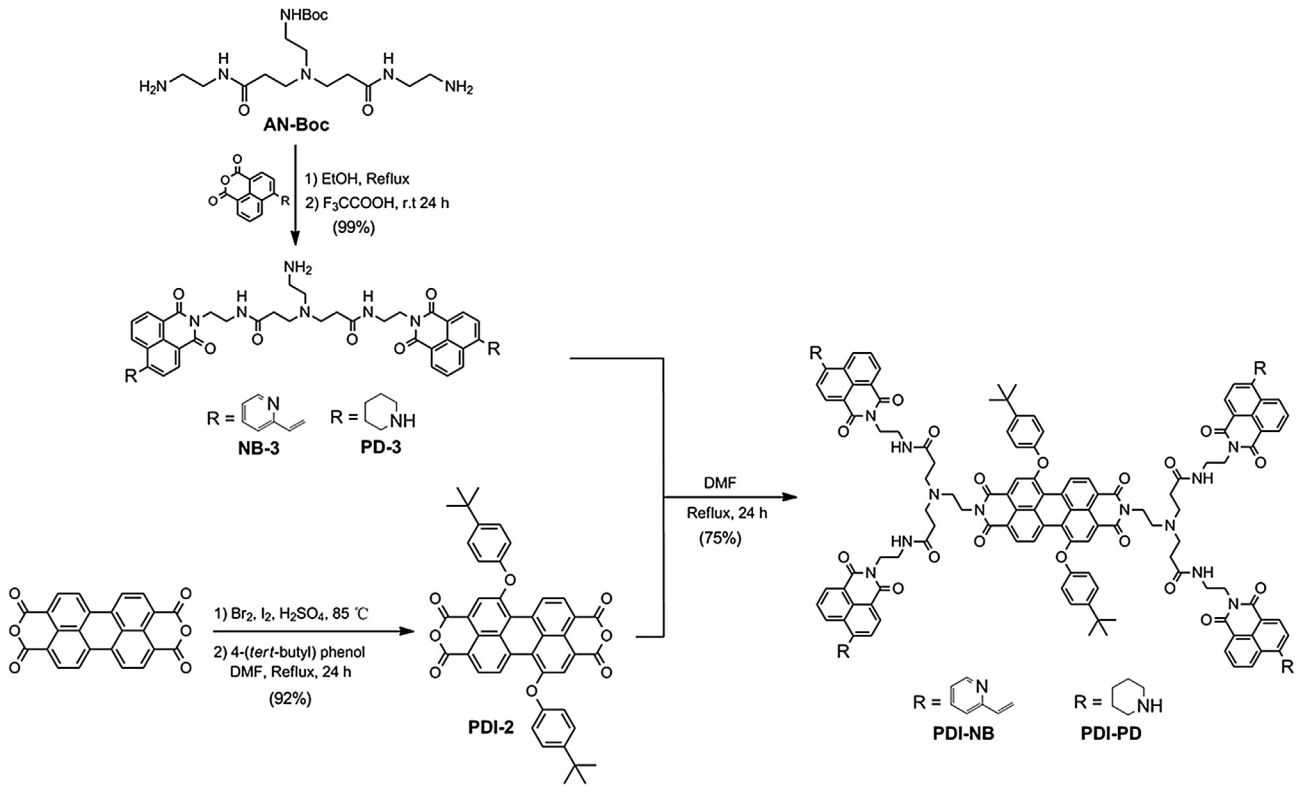

Scheme 2. Synthesis of perylenediimide–naphthalimide dendrons.

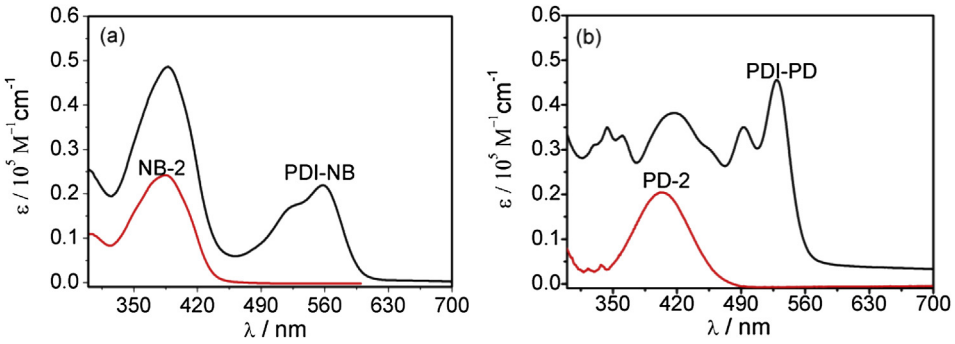

Fig. 2. Absorption spectra of **PDI-NB** (a) and **PDI-PD** (b) in H_2O/DMSO, 1:1.

fluorophore acceptor) would quench fluorescence emission of the perylenediimide unit [39–42]. The fluorescence spectra of **PDI-NB** and **PDI-PD** in DMSO/H_2O, obtained after excitation within the spectral region of maximal absorption of the peripheral fluorophore ($\lambda_{ex} = 385$ nm or 415 nm), showed two emission bands at 460/600 nm and 540/560 nm, corresponding to the emission bands of the donor 1, 8-naphthalimide derivates' fragments and the acceptor core in **PDI-NB** and **PDI-PD** as shown in Fig. 3. The corresponding data was showed in Table 1. The fluorescence quantum yield of **NB-2** units in **PDI-NB** was lower than that of compound **NB-2**. The weakened fluorescence emission may be caused by the electron transfer of N atom from of 4-replacing 1, 8-naphthalimide derivates [43–50]. On the other hand the fluorescence quantum yield of **PDI** units in **PDI-NB** was 0.07 which is nearly negligible as compared with the fluorescence quantum yield of compound **PDI-2**. Nearly same result can be obtained in probe **PDI-PD**. From the weakened fluorescence emission of perylenediimide unit in probe, it was predicted that a PET process (electron transfer from the nitrogen to the excited state of the **PDI** core or 1, 8-naphthalimide derivates) quenched fluorescence emission of the perylenediimide unit in **PDI-NB**.

In order to gain insight into the energy transfer process, the fluorescence life time was evaluated by additional fluorescence decay measurements. The fluorescence decay curves were showed in Fig. 4, which were measured by single photon counting method [51]. As showed in Table 1, the fluorescence life time of compound **PDI-NB** was 2.33 ns (at 450 nm) and 3.23 ns (at 600 nm), respectively. The fluorescence life time of compound **NB-2** was 4.9 ns (at 450 nm), this value was nearly two times that of the life of **NB** units in **PDI-NB**. The energy transfer rate constant for the Förster mechanism, K_{en}^{F}, can be estimated by using spectroscopic quantities and according to the equation (1) showed in the Supporting information [52]. The energy transfer rate constant was calculated to be 6.4×10^9 s^{-1} for **PDI-NB** and 5.2×10^9 s^{-1} for **PDI-PD**, respectively. The decreased value of fluorescence life of **NB-2** shows that the excited state energy transfer occurs to the **PDI** core in compound **PDI-NB**.

3.3. FRET of perylenediimide–naphthalimide dendrons based on Fe(III) or proton induced

Among biologically important metal ions, iron ion is an important microelement in the human body. It is an oxygen carrier in hemoglobin [53–55]. High doses of iron ions are, however, dangerous and can be toxic because of their ability to promote oxidation of lipids, proteins and other cellular components [56]. Due to the possible toxicity of iron ion, the design of fluorescent iron ion probes is an area of active investigation, and a great deal of effort has been devoted to the design of molecular receptors containing binding sites to iron ion [57–65].

As discussed above, the tertiary amines in space quenched the fluorescence emission of the perylenediimide unit in probes. The protonation or the respective metal coordination of the tertiary amines receptors would increase their oxidation potential, and as such, thermodynamically disallow the electron transfer [21,22,42]. Consequently electron transfer from the donors to the excited state of the fluorophore acceptor would be "switched off". Thus we expect the fluorescence signal of fluorophore serving as acceptor to be amplified.

As showed in Fig. 5(a) and (b), under excitation at $\lambda_{ex} = 385$ nm (within the maximal absorption of the peripheral fluorophore) the probe **PDI-NB** showed a subtle emission in the red-green spectral region, while fluorescence intensity of the donor–acceptor system **PDI-NB** with Fe^{3+} or H^+ induced in the same region is more than 8 times higher due to the energy transfer from the periphery to the focal chromophore. Fig. 5(a) and (b) represents the emission spectra of light harvesting antenna **PDI-NB** under excitation in periphery ($\lambda_{ex} = 385$ nm) and direct at the core ($\lambda_{ex} = 556$ nm). The

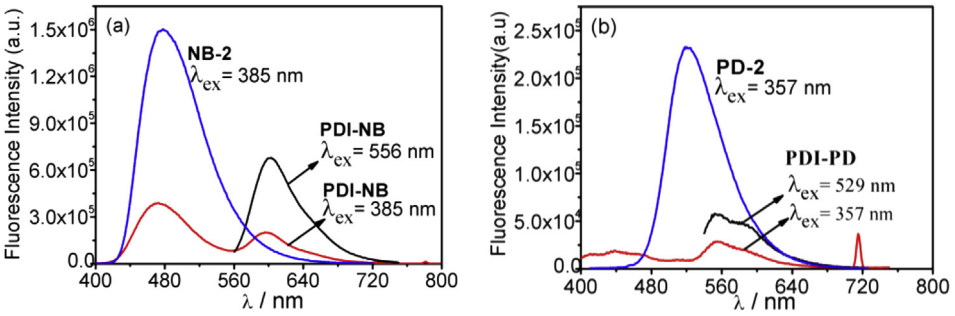

Fig. 3. Fluorescence spectra of **PDI-NB** (a) and **PDI-PD** (b) in H_2O/DMSO, 1:1.

Table 1
Optical properties of compounds **NB-2**, **PDI-NB** and **PDI-PD** in $CHCl_3$, 1/1 at 298 K.

Compounds	$\lambda_{labs}^{max}(\varepsilon_1)/\lambda_{2abs}^{max}(\varepsilon_2)$nm[a] ($10^5$ M^{-1} cm^{-1})[b]	$\lambda_{1flu}/\lambda_{2flu}$ (nm)[c]	$\Delta\nu_1/\Delta\nu_2$ (cm^{-1})[d]	Φ_1^{ex}/Φ_2^{ex}[e]	E_1/E_2 (%)[f]	τ_{1F}/τ_{2F} (ns)[g]
PDI-NB-Fe(III)	385(0.65)/556 (0.25)	460/600	4230/1313	0.01/0.24	98	–
PDI-NB	385(0.54)/556 (0.25)	460/600	4230/1313	0.55/0.07	–	2.33/3.23
NB-2	385 (0.48)	460	4230	0.76	–	4.9
PDI-PD-Fe(III)	415(0.65)/529 (0.25)	540/560	5571/6232	0.01/0.18	96	–
PDI-PD	415(0.54)/529 (0.25)	540/560	5571	0.56/0.09	–	4.6/4.04
PD-2	415 (0.48)	540	5571	0.72	–	5.2

The fluorescence quantum yields were determined using Quinoline ($\Phi = 0.55$ in sulfuric acid solution) and rhodamine 6G ($\Phi = 0.95$ in ethanol) as a standard. The max absorbance was used as the excited wavelength.
[a] Absorption maximum.
[b] The maximum molar extinction coefficients.
[c] Emission maximum.
[d] Stoke's shift $= (1/\lambda_{abs} - 1/\lambda_{em}) \times 10^7$.
[e] Fluorescence quantum yield.
[f] Energy transfer efficiency. $(\lambda, \Delta\nu, \Phi, E, \tau)_1$ = Naphthalimide unit in probe, $(\lambda, \Delta\nu, \Phi, E, \tau)_2$ = Perylenediimide unit in probe.
[g] The efficiency of energy transfer.

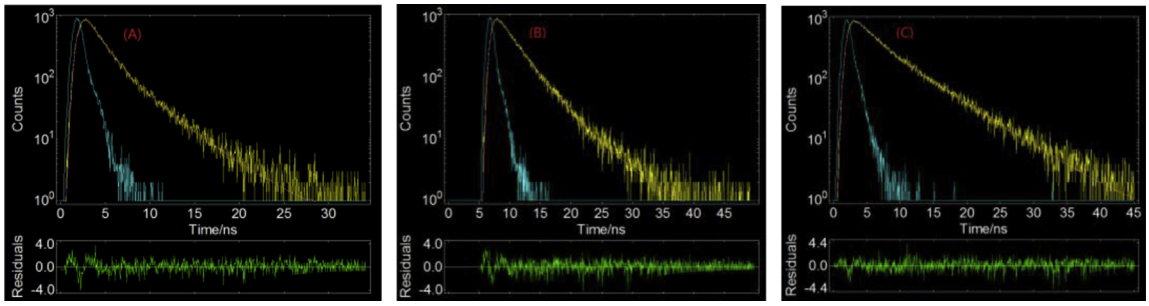

Fig. 4. Fluorescence decay curves of **PDI-NB** (a, b) and **NB-2** (c) in $CHCl_3$ at (A) 450 nm and (B) 600 nm and (C) 450 nm.

emission intensity of the core, excited by energy transfer from peripheral units ($\lambda_{ex} = 385$ nm), is 2 times higher than that of the one excited within the maximal absorption of the focal fluorophore ($\lambda_{ex} = 556$ nm). The difference between the harvested and direct core emissions clearly demonstrates the great ability of the light harvesting system **PDI-NB** with Fe^{3+} or H^+ induced to transfer energy from its periphery to the core. This observation indicates that the light harvesting antenna is more efficient than the core dye at capturing photons from environment. At the same time the emission intensity of the periphery in the light harvesting system **PDI-NB** was decreased by 98% as compared with the emission of the blue emitting reference 1, 8-naphthalimide at the same optical density. The efficiency of energy transfer was evaluated according to the equation: 100 × [1-(fluorescence intensity of the energy donor in the cassette)/(fluorescence intensity of the free energy donor)]% [66]. The same detection was conducted on **PDI-PD** (detailed data was showed in Table 1 in the Supporting information). Next, more detailed ratio detection was conducted as showed below.

The reason for fluorescence energy transfer of **PDI-NB** and **PDI-PD** with Fe(III) or H^+ induced could be the possible photoinduced electron transfer (PET) from the PAMAM bone to the core of probe (**PDI-NB** and **PDI-PD**) as shown in Fig. 6. The poly(amidoamine) architecture contains a tertiary amine proton receptor able to involve the system in a PET process. In this particular probe, it was predicted that the PET process (an electron transfers from the receptor to the excited state of the fluorophore) would quench fluorescence emission of the perylenediimids units. The protonation of the tertiary amine in the fluorophore-amine conjugates would increase the oxidation potential of the receptor. Thus, we expect the fluorescence signal of the light **PDI-NB** and **PDI-PD** to be a function of Fe(III) or proton.

Fluorescence increase of the light harvesting dendrons **PDI-NB** and **PDI-PD** as a function of Fe(III) and pH concentration were observed only under excitation within the spectral region of maximal absorption of the peripheral fluorophores. This is an indication of the two amine receptors' involvement in PET quenching of the perylenediimid core's excited state. Upon

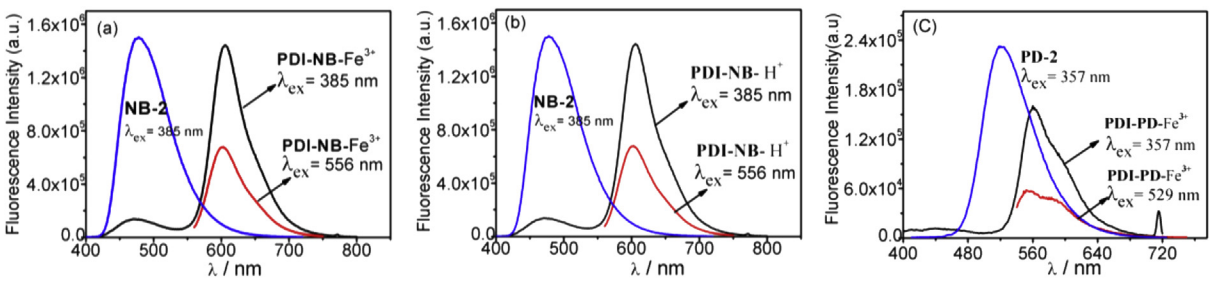

Fig. 5. FRET based fluorescence spectra of (a) **PDI-NB**-Fe(III), (b) **PDI-NB**-H^+ and (c) **PDI-PD**-Fe(III) in water (DMSO/H_2O, 1:1, v/v) ($c = 10$ μM).

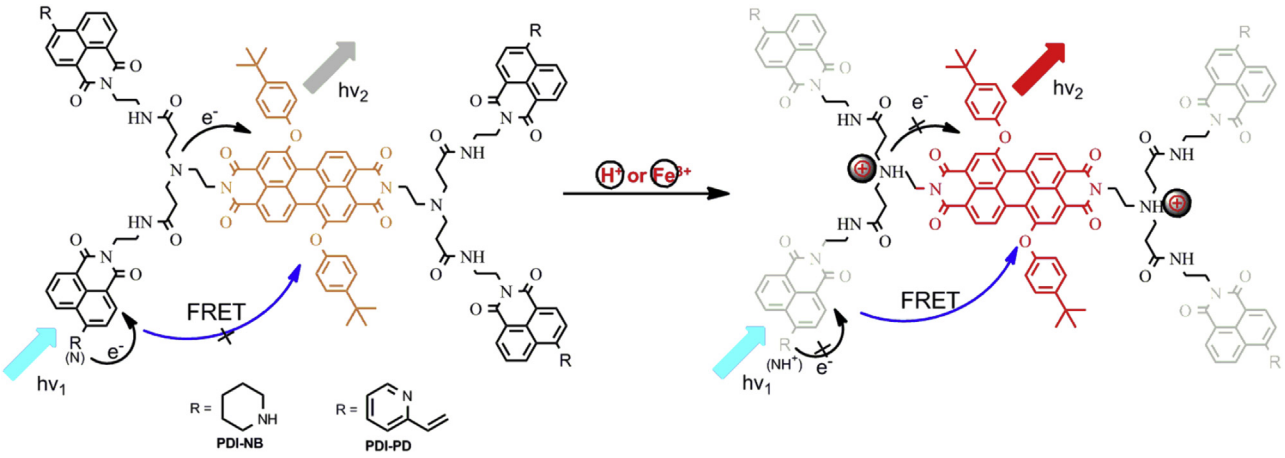

Fig. 6. The possible binding mode of dyes with Fe(III) or H^+.

protonation or bonding with Fe(III) of this amine the quenching process is substantially removed.

3.4. FRET efficiency of the probes as a function of Fe(III) concentration

The Fe(III)-binding behaviors of fluorescent probes **PDI-NB** and **PDI-PD** were investigated by absorption and fluorescence spectroscopy. Fluorescent probe **PDI-NB** displays weak fluorescence with a fluorescence quantum yield of 8% in DMSO/H_2O (1:1, v/v). But this probe shows significant enhancement of fluorescence upon the addition of Fe(III), which leads to a fluorescent increase by 20-fold at 600 nm (Fig. 7(a)). The titration curve of fluorescent probe **PDI-NB** to the concentration of Fe(III) ions shows that with the concentration of Fe(III) ions enhanced from 2 μM to 20 μM there are significant increases in fluorescence intensity (at 600 nm), followed by a negligible increase in fluorescent intensity with the concentrations of Fe(III) ions at 24 μM and higher (Fig. 7(a)-inset). This suggests that the binding of 20 μM Fe(III) ions to **PDI-NB** (10 μM) is close to saturation, and that fluorescent probe **PDI-NB** interacts with Fe(III) in 2 equivalent molar ratio. At the same time the probe shows significant absorption increases at 385 nm upon the addition of Fe(III) accompanied by a blue shift in the absorption spectrum (Fig. 8(a)). The hypsochromic shift is due to the weakened electron-

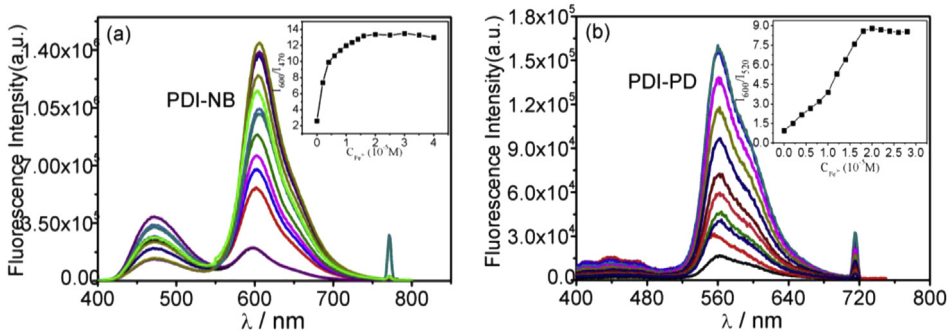

Fig. 7. Fluorescence spectra of **PDI-NB** and **PDI-PD** in H_2O/DMSO (c = 10 μM, $\lambda_{PDI\text{-}NB}$ = 385 nm, $\lambda_{PDI\text{-}PD}$ = 357 nm) in the presence of Fe(III) at concentration of 2–40 μM. Inset: Relative fluorescent intensities of I_{accept}/I_{donor} as a function of Fe(III) concentration).

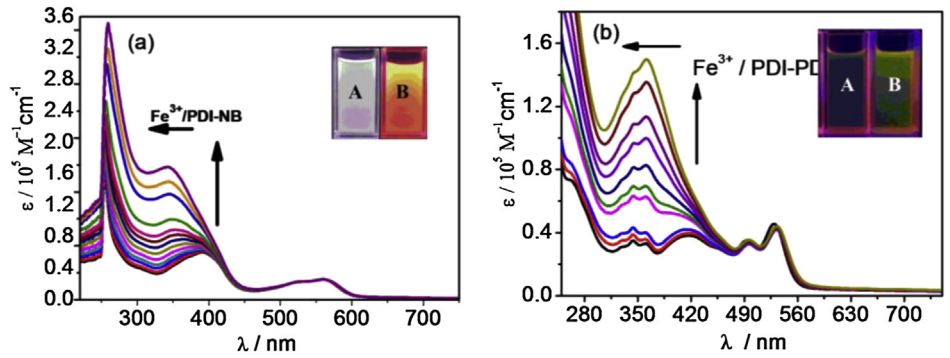

Fig. 8. Absorption spectra of **PDI-NB** (a) and **PDI-PD** (b) as a function of Fe(III) concentration ([**PDI-NB**] = 10 μM. Inset: Color change of **PDI-NB** and **PDI-PD** (10 mM) on the addition of 40 eq. of Fe(III) or proton under lamp 365 nm, A = probe, B = probe-Fe(III) or proton).

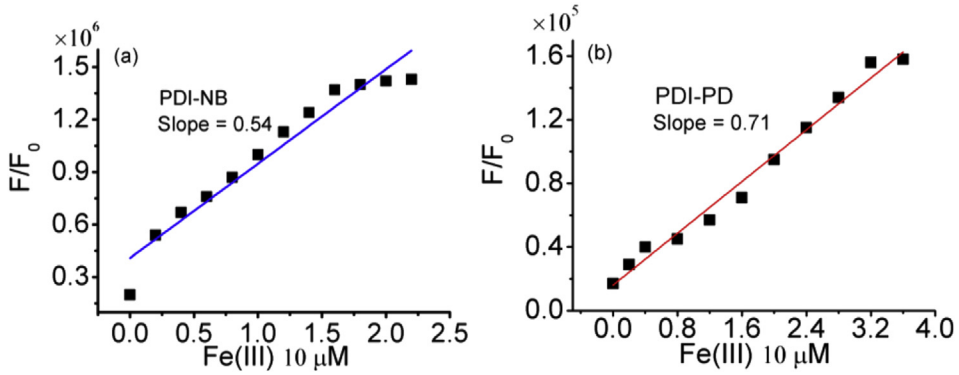

Fig. 9. The linear relationship between the fluorescence intensity of probes and Fe(III) in concentration within the range 2–40 μM.

donor ability of the nitrogen atom at pyridine units whose electron couple is engaged in the complex formation with Fe(III) ions.

Fluorescent probe **PDI-PD** displays weaker fluorescence than probe **PDI-NB** with a fluorescence quantum yield of 5% in DMSO/H_2O (1:1, v/v). This is due to more efficient fluorescence quenching by photo-induced electron transfer from two tertiary amine groups to the BODIPY core of the probe **PDI-PD** as compared to the tertiary amine group of the probe **PDI-NB**. It displays similar responses to Fe(III) ions in its absorption and fluorescence spectra as fluorescent probe **PDI-NB**. Fluorescent probe **PDI-PD** shows increased blue shifts in absorption spectra compared to fluorescent probe **PDI-NB** and the addition of 20 μM Fe(III) ions to fluorescent probe **PDI-PD** led to 50 nm blue shift in the absorption spectrum at 415 nm (Fig. 8(b)).

3.5. Dissociation constant and the detection limit of probes

The apparent dissociation constant (K_d) was obtained by direct fluorometric titration as a function of Fe(III) (in DMSO/H_2O) using the fluorescence emission spectra according to the reported method [67]. The fluorescence intensity data (Fig. 9) was fitted to eqn (1): F_{min} and F_{max} are the emission intensities with no addition of Fe(III) and an addition of Fe(III) at 600 nm, respectively; n is the binding stoichiometry between **PDI-NB** and Fe(III). A 2:1 stoichiometry between probe and Fe(III) was assumed, and then the binding stoichiometry kept fixed at 2 in the final curve fittings, The value of K_d was found to be 5.3×10^{-11} M for **PDI-NB** and 2.5×10^{-10} M for **PDI-PD**.

$$F = \frac{F_{min}K_d + F_{max}[X]^n}{K_d + [X]^n} \quad (1)$$

The detection limit and quantification limit were measured to be 1.2×10^{-7} M for **PDI-NB** (3σ/slope, σ is the standard deviation of the blank measurement) [68] and 1.8×10^{-7} M for **PDI-PD**, respectively. In addition, the interaction of probes with Fe(III) was completed in a few seconds, therefore 1 could be used for the real-time and real-space analysis of Fe(III) ions, These results proved that the probes possess a remarkably high binding affinity and sensitivity to Fe(III).

3.6. FRET efficiency of the probes at various pH values

Protons play critical roles [69–71] in many cellular events such as cell growth and apoptosis, calcium regulation, etc. So, protons have become one of the most important sensing targets among the interesting species [72]. According to published reports [39–42], the fluorescence emission of PAMAM dendrons based on 1, 8-naphthalimide is efficient "off–on" switcher for pH. The novel light harvesting systems **PDI-NB** and **PDI-PD** are designed just based on this theory. This was the reason to investigate the photophysical behavior of **PDI-NB** and **PDI-PD** at different pH values.

The pH dependence of the fluorescence properties of dendrimer **PDI-NB** as a function of pH in water/DMSO (1:1, v/v) is illustrated in Fig. 10(a). Weak fluorescence was observed at pH 8.00 with an excitation wavelength of 385 nm. However, as the pH decreased from 8.0 to 6.0, emission band centered at 600 nm increased gradually and a distinct emission enhancement was observed with the change of fluorescence intensity over 10-fold. The fluorescence quantum yield of **PDI-NB** was also measured. In pH 10.0, the fluorescence intensity was very low ($\Phi = 0.07$) relative to rhodamine B ($\Phi = 0.95$ in MeOH) [73]. But when the pH was decreased to 6.00, strong fluorescence was obtained immediately with a higher

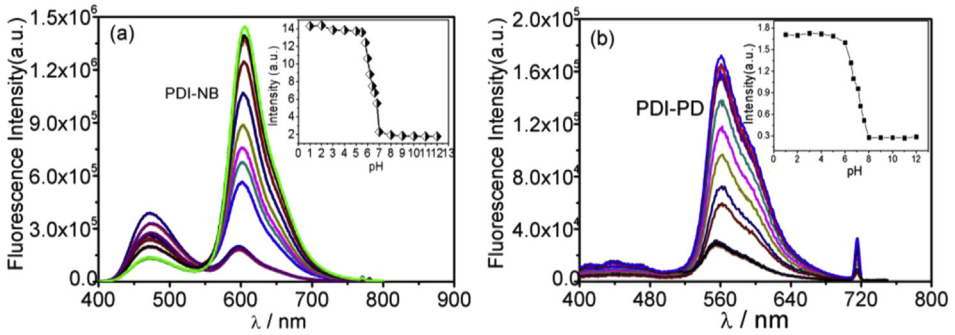

Fig. 10. Fluorescence spectra of **PDI-NB** (a) and **PDI-PD** (b) at various pH values ($c = 10$ μM, $\lambda_{PDI\text{-}NB} = 385$ nm, $\lambda_{PDI\text{-}PD} = 357$ nm). Inset: Relative fluorescent intensities of I_{accept}/I_{donor} in pH = 1–13.

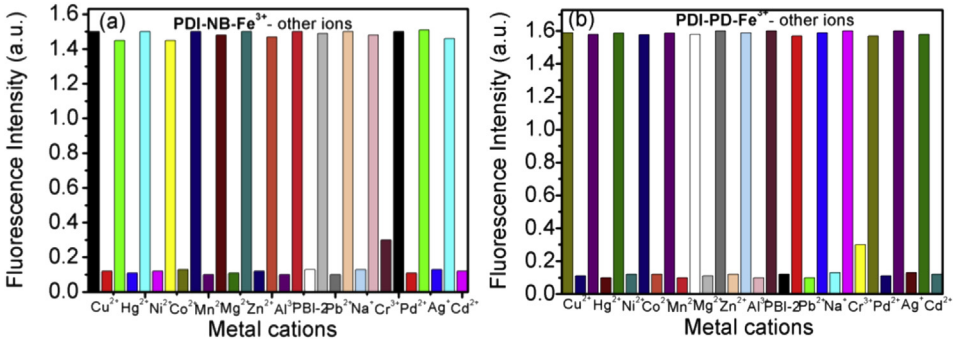

Fig. 11. Fluorescence responses of probe molecules to various metal ClO_4^- salts of metal cations such as K^+, Fe^{3+}, Ca^{2+}, Mg^{2+}, Mn^{2+}, Cr^{3+}, Al^{3+} and Co^{2+} (3 eq.).

fluorescence quantum yield (Φ) of 0.24. Nearly same result can be obtained in probe **PDI-PD** (Fig. 10(b)). These changes are of such magnitude that they can be considered as a pH "ON–OFF", where the fluorescence emission is "switched off" in alkaline solution and "switched on" in acidic solution.

The light harvesting systems **PDI-NB** and **PDI-PD** are thus efficient "off–on" switcher for pH. This switching process was also found to be reversible. Taking the part of the graph in Fig. 5 located between pH 3 and 9, the pKa values of the light harvesting dendron **PDI-NB** and **PDI-PD** have been calculated by Eq. (2) [41]. The calculated pKa value for **PDI-NB** was 6.02 and 6.25 for **PDI-PD**. These results proved that the probes possess a high binding affinity and sensitivity to proton.

$$\mathrm{Log}[I_{F\max} - I_F/I_F - I_{F\min}] = \mathrm{pH} - \mathrm{pKa} \quad (2)$$

3.7. Interference of metal cations in the fluorescence intensity of dyes

Interference experiments with additional metal ions were taken into account. As illustrated in Fig. 11, The probe exhibits poor selectivity towards Cr(III), No significant response of fluorescent probes **PDI-NB** and **PDI-PD** was observed in the presence of 10 mM other metal ions such as Na^+, K^+, Ca^{2+}, Mg^{2+}, Co, Ni^{2+}, Cu^{2+}, Zn^{2+}, Mg^{2+}, Pd^{2+}, Pb^{2+}, Fe^{2+}, Mn^{2+} and Al^{3+} ions.

4. Conclusions

In summary, two novel "switched on" fluorescent probes (**PDI-NB** and **PDI-PD**) with **PDI** as the fluorophore were successfully prepared, and fully characterized by ^{1}H NMR, ^{13}C NMR and HRMS-MALDI-TOF. The probes exhibited high selectivity toward Fe(III) in the presence of various other metal cations and sensitivity to proton. A 1:2 stoichiometry was found for the complex formed by probes and Fe(III). The probes possess a remarkably high binding affinity and sensitivity to Fe(III) and proton according to the obtained dissociation constant and the detection limit of the probes. **PDI-NB** and **PDI-PD** present abilities of fast fluorescence detection of Fe(III) and proton with high energy transfer efficiency of 96–98%. In response to Fe(III) ions, **PDI-NB** demonstrated remarkable fluorescence intensity change and also sharp color change from pink to bright yellow in ultraviolet light. The obvious absorption and fluorescence variation upon the addition of Fe(III) ion can be observed both by naked eyes and by optical responses. The result of our research suggests that these off–on-type fluorescence probes for metal ions or proton-dependent on PET-FRET progress are efficient. Considering the multitude of choices for the structure modification of **PDI**, we are convinced that the design strategy will help to develop a new class of excellent **PDI**-based dendrimers with practical application in many sensing fields, such as environmental research and biology.

Acknowledgments

This work was financially supported by the Fundamental Research Funds for the National Natural Science Foundation of China (No. 61178057) and for the Central Universities (No. CXLX12_0085).

Appendix A. Supplementary data

Supplementary data related to this article can be found at http://dx.doi.org/10.1016/j.dyepig.2014.07.005.

References

[1] Wasielewski MR. Energy, charge, and spin transport in molecules and self-assembled nanostructures inspired by photosynthesis. J Org Chem 2006;71:5051–66.
[2] Elemans JAA, van Hameren R, Nolte RJM, Rowan AE. Molecular materials by self-assembly of porphyrins, phthalo-cyanines, and perylenes. Adv Mater 2006;18:1251–66.
[3] WÜrthner F. Perylene bisimide dyes as versatile building blocks for functional supramolecular architectures. Chem Commun 2004:1564–79.
[4] Zhang J, Fischer MKR, Bäuerle P, Goodson T. Energy migration in dendritic oligothiophene-perylene bisimides. J Phys Chem B 2013;117(16):4204–15.
[5] Bozdemir OA, Yilmaz MD, Buyukcakir O, Siemiarczuk A, Tutasd M, Akkay EU. Convergent synthesis and light harvesting properties of dendritic boradiazaindacene (BODIPY) appended perylenediimide dyes. New J Chem 2010;34:151–5.
[6] Matthew MS, Chun H, Ariel SM, Nikolay M, Stephen B, Seth RM, et al. Nonlinear optical pulse suppression via ultrafast photoinduced electron transfer in an aggregated perylene diimide/oligothiophene molecular triad. J Phys Chem A 2014;118:110–21.
[7] Hahn U, Nierengarten JF, Delavaux-Nicot B, Monti F, Chiorbolid C, Armaroli N. Fullerodendrimers with a perylenediimide core. New J Chem 2011;35:2234–44.
[8] Yilmaz MD, Bozdemir OA, Akkaya EU. Light harvesting and efficient energy transfer in a boron-dipyrrin (BODIPY) functionalized perylenediimide derivative. Org Lett 2006;8(13):2871–3.
[9] Feng J, Liang B, Wang D, Xue L, Li X. Novel fluorescent dyes with fused perylene tetracarboxlic diimide and BODIPY analogue structures. Org Lett 2008;10:4437–40.
[10] Zhao C, Zhang Y, Li R, Li X, Jiang J. Di(alkoxy)- and di(alkylthio)-substituted perylene-3,4:9,10-tetracarboxy diimid-es with tunable electrochemical and photophysical properties. J Org Chem 2007;72:2402–10.
[11] Xu W, Chen H, Wang Y, Zhao C, Li X, Wang SY. Photoinduced electron and energy transfer in dyads of porphyrin dimer and perylene tetracarboxylic diimide. Chem Phys Chem 2008;9:1409–15.
[12] Jones BA, Ahrens MJ, Yoon MH, Facchetti A, Marks TJ, Wasielewski MR. High-mobility air-stable n-type semiconductors with processing versatility: dicyanoperylene-3,4:9,10-bis(dicarboximides). Angew Chem Int Ed 2004;43:6363–6.
[13] Liu XJ, Zhang N, Zhou J, Chang TJ, Fang CL, Shang DH. A turn-on fluorescent sensor for zinc and cadmium ions based on perylene tetracarboxylic diimide. Analyst 2013;138:901–6.
[14] Chen XQ, Jou MJ, Yoon JY. An "Off–On" type UTP/UDP selective fluorescent probe and its application to monitor glycosylation process. Org Lett 2009;11(10):2181–4.

[15] Ruan YB, Li AF, Zhao JS, Shen JS, Jiang YB. Specific Hg^{2+}-mediated perylene bisimide aggregation for highly sensitive detection of cysteine. Chem Commun 2010;46:4938–40.
[16] Szelke H, SchubeL S, Harenberg J, Kramer R. A fluorescent probe for the quantification of heparin in clinical samples with minimal matrix interference. Chem Commun 2010;46:1667–9.
[17] Yang Y, Li WY, Qi H, Zhang QF, Chen J, Wang Y, et al. Detection of silver(I) ions based on the controlled self-assembly of a perylene fluorescence probe. Anal Biochem 2012;430:48–52.
[18] Wang B, Wang FY, Jiao HP, Yang XY, Yu C. Label-free selective sensing of mercury(II) via reduced aggregation of the perylene fluorescent probe. Analyst 2010;135:1986–91.
[19] Wang B, Zhu QK, Liao DL, Yu C. Perylene probe induced gold nanoparticle aggregation. J Mater Chem 2011;21:4821–6.
[20] Wang B, Jiao HP, Li WY, Liao DL, Wang FY, Yu C. Superquencher formation via nucleic acid induced noncovalent perylene probe self-assembly. Chem Commun 2011;47:10269–71.
[21] Liu K, Xu Z, Yin MZ, Yang W, He B, Wei W, et al. A multifunctional perylenediimide derivative (DTPDI) can be used as a recyclable specific Hg^{2+} ion sensor and an efficient DNA delivery carrier. J Mater Chem B 2014;2:2093–6.
[22] Georgiev NI, Sakr AR, Bojinov VB. Design and synthesis of novel fluorescence sensing perylene diimides based on photoinduced electron transfer. Dyes Pigments 2011;91:332–9.
[23] Hurenkamp JH, Browne WR, Augulis R, Pugzlys A, Feringa BL. Intramolecular energy transfer in a tetra-coumarin perylene system: influence of solvent and bridging unit on electronic properties. Org Biomol Chem 2007;5:3354–62.
[24] Chen CT, Huang WP. A highly selective fluorescent chemosensor for lead ions. J Am Chem Soc 2002;124:6246–7.
[25] Kim JS, Quang DT. Calixarene-derived fluorescent probes. Chem Rev 2007;107:3780–99.
[26] Chen CT, Huang WP. Tools and tactics for the optical detection of mercuric ion. J Am Chem Soc 2002;124:6246–7.
[27] Huang J, Xu Y, Qian X. A rhodamine-based Hg^{2+} sensor with high selectivity and sensitivity in aqueous solution: a NS2-containing receptor. J Org Chem 2009;74:2167–70.
[28] Tsien RY, Miyawaki A. Seeing the machinery of live cells. Science 1998;280:1954–5.
[29] Weiss S. Fluorescence spectroscopy of single biomolecules. Science 1999;283(5408):1676–83.
[30] De Silva AP, Gunnlaugsson T, Rice TE. Recent evolution of luminescent photoinduced electron transfer sensors. Analyst 1996;121:1759–62.
[31] De Silva AP, Gunaratne HQN, McCoy CP. Direct visual indication of pH windows: "off–on–off" fluorescent PET (photoinduced electron transfer) sensors/switches. Chem Commun 1996:2399–400.
[32] Krämer R. Fluorescent chemosensors for Cu^{2+} ions: fast, selective, and highly sensitive. Angew Chem Int Ed 1998;37:772–3.
[33] Fabbrizzi L, Licchelli M, Parodi L, Poggi A, Taglietti1 AJ. The molecular design of fluorescent sensors for ionic analytes. J Fluoresc 1998;8:263–71.
[34] Wiskur SL, Ait-Haddou H, Lavigne JJ, Anslyn EV. Teaching old indicators new tricks. Acc Chem Res 2001;34:963–72.
[35] Wang HX, Wang DL, Wang Q, Li XY, Schalley CA. Nickel(II) and iron(III) selective off–on-type fluorescence probes based on perylene tetracarboxylic diimide. Org Biomol Chem 2010;8:1017–26.
[36] McKenna MD, Grabchev I, Bosch P. The synthesis of a novel 1,8-naphthalimide based PAMAM-type dendron and its potential for light-harvesting. Dyes Pigments 2009;81:180–5.
[37] Dai HL, Yan Y, Guo Y, Fan LL, Che ZP, Xu H. A selective and sensitive "Turn-on" fluorescent chemosensor for recognition of Hg^{2+} ions in water. Chem Eur J 2012;18:11188–91.
[38] Ahrens MJ, Tauber MJ, Wasielewski MR. Bis(n-octylamino)perylene-3,4:9,10-bis(dicarboximide)s and their radial cations: synthesis, electrochemistry, and ENDOR spectroscopy. J Org Chem 2006;71:2107–44.
[39] Georgiev NI, Bojinov VB, Nikolov PS. Design and synthesis of a novel pH sensitive core and peripherally 1,8-naphthalimide-labeled PAMAM dendron as light harvesting antenna. Dyes Pigments 2009;18:18–26.
[40] Georgiev NI, Bojinov VB, Marinova N. Novel PAMAM light-harvesting antennae based on 1,8-naphthalimide: synthesis, energy transfer, photophysical and pH sensing properties. Sensors Actuat B 2010;150:655–66.
[41] Staneva D, Bosch P, Asiri AM, Taib LA, Grabchev I. Studying pH dependence of the photophysical properties of a blue emitting fluorescent PAMAM dendrimer and evaluation of its sensor potential. Dyes Pigments 2014;105:114–20.
[42] Grabcheva I, Bosch P, Staneva D. A new detector for metal cations based on the combined effect of photoinduced electron transfer and a light harvesting system. J Photochem Photobiol Chem 2011;222:288–92.
[43] Marinova NV, Georgiev NI, Bojinov VB. Design, synthesis and pH sensing properties of novel 1,8-naphtalimide-based bichromophoric system. J Photochem Photobiol Chem 2011;222:132–40.
[44] Shang HX, Luo YH, Guo XZ, Huang XM, Zhan XW, Jiang KJ, et al. The effect of anchoring group number on the performance of dye-sensitized solar cells. Dyes Pigments 2010;87:249–56.
[45] Georgiev Nikolai I, Bojinov Vladimir B. Design, synthesis and photostability of novel 1,8-naphthalimide PAMAM light-harvesting dendrons. J Fluoresc 2011;21:51–63.
[46] Georgiev NI, Bryaskova R, Tzoneva R, Ugrinova I, Detrembleur C, Miloshev S, et al. A novel pH sensitive water soluble fluorescent nanomicellar sensor for potential biomedical applications. Bioorg Med Chem 2013;21:6292–302.
[47] Georgiev NI, Asiri AM, Qusti AH, Alamry KA, Bojinov VB. Design and synthesis of pH-selective fluorescence sensing PAMAM light-harvesting dendrons based on 1,8-naphthalimides. Sensors Actuat B 2014;190:185–98.
[48] Georgiev NI, Bojinov VB, Venkova AI. Design, synthesis and pH sensing properties of novel PAMAM light-harvesting dendrons based on rhodamine 6G and 1,8-naphthalimide. J Fluoresc 2013;23:459–71.
[49] Georgiev NI, Asiri AM, Qusti AH, Alamry KA, Bojinov VB. A pH sensitive and selective ratiometric PAMAM wavelength-shifting bichromophoric system based on PET, FRET and ICT. Dyes Pigments 2014;102:35–45.
[50] Georgiev NI, Dimov SM, Asiri AM, Alamry KA, Obaid AY, Bojinov V. Synthesis, selective pH-sensing activity and logic behavior of highly water-soluble 1,8-naphthalimide and dihydroimidazonaphthalimide derivatives. J Lumin 2014;149:325–32.
[51] Wang XM, Jin F, Chen ZG, Liu SQ, Wang XH, Duan XM, et al. A new family of dendrimers with naphthaline core and triphenylamine branching as a two-photon polymerization initiator. J Phys Chem C 2011;115:776–84.
[52] Forster T. 10th spiers memorial lecture transfer mechanisms of electronic excitation. Disc Faraday Soc 1959;27:7–17.
[53] Aisen P, Wessling-Resnick M, Leibold EA. Iron metabolism. Curr Opin Chem Biol 1999;3:200–6.
[54] Eisenstein RS. Iron regulatory proteins and the molecular control of mammalian iron metabolism. Annu Rev Nutr 2000;20:627–32.
[55] Rouault TA. The role of iron regulatory proteins in mammalian iron homeostasis and disease. Nat Chem Biol 2006;2:406–14.
[56] Lee MH, Giap TV, Kim SH, Lee YH, Kang C, Kim JS. A novel strategy to selectively detect Fe(III) in aqueous media driven by hydrolysis of a rhodamine 6G Schiff base. Chem Commun 2010;46:1407–9.
[57] Huang L, Hou FP, Cheng J, Xi PX, Chen FJ, Bai DC, et al. Selective off–on fluorescent chemosensor for detection of Fe^{3+} ions in aqueous media. Org Biomol Chem 2012;10:9634–8.
[58] Wu SP, Chen YP, Sung YM. Colorimetric detection of Fe^{3+} ions using pyrophosphate functionalized gold nanoparticles. Analyst 2011;136:1887–91.
[59] Xu HJ, Liu ZD, Sheng LQ, Chen MM, Huang DQ, Zhang H, et al. A novel "turn-on" fluorescent probe for Fe^{3+} in aqueous media based on C=N isomerization. New J Chem 2013;37:274–7.
[60] Qu XY, Liu Q, Ji XN, Chen HC, Zhou ZK, Shen Z. Enhancing the Stokes' shift of BODIPY dyes via through-bond energy transfer and its application for Fe^{3+}-detection in live cell imaging. Chem Commun 2012;48:4600–2.
[61] Shellaiah M, Wu YH, Singh A, Ramakrishnam MV, Lin HC. Electrochemical synthesis and photocatalytic property of cuprous oxide nanoparticles. J Mater Chem A 2013;1:1310–8.
[62] Liu RL, Lu HY, Li M, Hu SZ, Chen CF. Simple, efficient and selective colorimetric sensors for naked eye detection of Hg^{2+}, $Cu^{2+}$and Fe^{3+}. RSC Adv 2012;2:4415–20.
[63] Bhalla V, Gupta A, Kumar M. A pentacenequinone derivative with aggregation-induced emission enhancement characteristics for the picogram detection of Fe^{3+} ions in mixed aqueous media. Dalt Trans 2013;42:4464–9.
[64] Renukamal V, Paula K, Kumar S. A dual-responsive chromo-fluorescent probe for detection of Zn^{2+} and Fe^{3+} via two different approaches. RSC Adv 2013;3:9189–92.
[65] Dang S, Ma E, Sun ZM, Zhang HJ. A layer-structured Eu-MOF as a highly selective fluorescent probe for Fe^{3+} detection through a cation-exchange approach. J Mater Chem 2012;22:16920–6.
[66] Jiao GS, Loudet A, Lee HB, Kalinin S, Johanssonb LBA, Burgess K. Syntheses and spectroscopic properties of energy transfer systems based on squaraines. Tetrahedron 2003;59:3109–16.
[67] Baruah M, Qin WW, Vallèe RA, Rohand T, Dehaen W, Boens N. A highly potassium-selective ratiometric fluorescent indicator based on BODIPY aza-crown ether excitable with visible light. Org Lett 2005;7:4377–80.
[68] Chen mL, Xin L, Liu YL, Zhao Y, Liu J, Wang P, et al. An 2-(2′-aminophenyl) benzoxazole-based OFF–ON fluorescent chemosensor for Zn^{2+} in aqueous solution. Org Biomol Chem 2011;9:2345–9.
[69] Gottlieb RA, Nordberg JE, Babior BM. Apoptosis induced in Jurkat cells by several agents is preceded by intracellular acidification. Proc Natl Acad Sci U S A 1996;93:654–8.
[70] Golovina VA, Blaustein MP. Spatially and functionally distinct Ca^{2+} stores in sarcoplasmic and endoplasmic reticulum. Science 1997;275:1643–8.
[71] Paradiso AM, Tsien RY, Machen TE. Digital image processing of intracellular pH in gastric oxyntic and chief cells. Nature 1987;325:447–50.
[72] Han J, Burgess K. Fluorescent indicators for intracellular pH. Chem Rev 2010;110:2709–28.
[73] Demas JN, Crosby GA. The measurement of photoluminescence quantum yields. J Phys Chem 1971;75:991–1024.